# Analysis and evaluation of the maximum throughput for data streaming over IEEE 802.15.4 wireless networks

Konstantin Mikhaylov[a,*], Jouni Tervonen[a]

[a] *Oulu Southern Institute, University of Oulu, Vierimaantie 5, 84100 Ylivieska, Finland; E-Mails: {konstantin.mikhaylov, jouni.tervonen}@oulu.fi*

* *Author to whom correspondence should be addressed; E-Mail: konstantin.mikhaylov@oulu.fi; Tel.: +358-468-841-370.*

**Abstract**. Recently, multiple novel applications have been developed using IEEE 802.15.4-based radio modules. In this paper, we focus on the maximum throughput that one can obtain with IEEE 802.15.4-based transceivers that operate in the license-free 2.4 GHz band using the 2450 direct-sequence spread spectrum physical layer. The results of the thorough maximum throughput analysis for single-hop and multi-hop data streaming scenarios in the beacon-enabled (with both contention access and contention-free periods) and nonbeacon-enabled networks are presented. The results of the analysis are compared with the results of the experiments, which were performed using contemporary IEEE 802.15.4 hardware transducers. Aside from defining the maximum possible throughput for the different scenarios, the presented data disclose the effect of various parameters on communication throughput and latency. The presented results reveal the capabilities of the IEEE 802.15.4 technology and enable one to estimate the feasibility of using the technology for particular applications.

**Keywords:** IEEE 802.15.4, 2450 DSSS, throughput, capacity, latency, beacon-enabled, CAP, CFP, analysis, evaluation, measurement

## 1. Introduction

The first revision of the IEEE 802.15.4 standard was introduced in 2003. The major purpose for the development of the standard was to provide a solution that was low in complexity, cost, power consumption and data rate to provide wireless connectivity among inexpensive devices [32]. Since its introduction, the specifications have been widely used and became the de-facto standard for communication for general-purpose wireless sensor and actuator networks (WSANs)[23]. Although throughput was not considered among the most important features of the IEEE 802.15.4, some of the current IEEE 802.15.4-based applications require high throughput. In this paper, we focus on the maximum throughput that one can obtain in IEEE 802.15.4 networks during data streaming with the unidirectional transmission of multiple sequential data frames with minimum interframe delay from a single transmitter to a single receiver. Note that the WSAN communication technologies are restricted in the size of the transmitted data frames. Therefore, the need to stream data arises each time that the size of the data to be transmitted is significantly higher than the maximum single frame payload. Among real-life WSAN applications that require data streaming are:

- transmission of an image, a sound record or real-time audio clip in wireless multimedia sensor networks [2,21,24];
- transmission of an electrocardiography (ECG) record, of an electroencephalography(EEG) record or of an image in biomedical sensor networks or body area networks [14];

- over-the-air reprogramming or another service operation with WSAN nodes [6,25];
- data transfer from isolated nodes to the mobile ferry [12,20,28].

Determination of the maximum throughput supported by the standard and a clear understanding of how the communication parameters affect the throughput are essential to understanding the capabilities of the IEEE 802.15.4-based system and enabling estimation of the feasibility of using the standard-based transceivers for a particular application. Therefore, we study the maximum throughput one can obtain with IEEE 802.15.4 transceivers operating in the license-free industrial, scientific and medical (ISM) 2.4 GHz band utilizing the 2450 direct-sequence spread spectrum (DSSS) physical layer in the paper. The major contributions of our work are providing **analytic** and **experimental results** that reveal the maximum throughput possible for single-hop and multi-hop data streaming in **all** possible IEEE 802.15.4 operation modes (i.e., the beacon-enabled with transmission in a contention access period (CAP), the beacon-enabled with transmission in CAP and contention-free periods (CFP), the nonbeacon-enabled). The presented results reveal the effects of the communication parameters and of the hardware features on data link throughput and latency.

In the following sections, we first discuss some of the previous research focused on IEEE 802.15.4 throughput in Section 2. In Section 3, we provide a brief overview of the IEEE 802.15.4 protocol. Section 4 presents the analytic results for IEEE 802.15.4 data transfer in different operation modes and introduces the formulas that describe the maximum throughput. Then, Section 5 discusses the details of the experiments executed using real-life IEEE 802.15.4 transceivers and presents the obtained results. Finally, Section 6 concludes the paper and summarizes the results.

## 2. Related work

During the ten years that have passed since the introduction of the IEEE 802.15.4 standard, multiple papers discussing the throughput of the standard have been published.

In their work, Sun et al. [27] noted that for the single-hop scenario, the upper bound of the effective throughput in the IEEE 802.15.4 nonbeacon-enabled network is defined by the sum of time required for the transmission of frame header, data, acknowledgement (if required) and wait period between frames (i.e., interframe space (IFS)). According to their analysis, the maximum effective throughput for unacknowledged single-hop data transmission is 140.9 kb/s. Nonetheless, the authors do not consider that some service operations (e.g., carrier sense multiple access (CSMA) algorithm or radio switching between receive (RX) and transmit (TX) modes) can be executed during the IFS. As a result, their estimation of maximum effective throughput is understated.

In [15] and [7], the authors fix this omission and consider the possibility of running the CSMA algorithm during the IFS. In [15], Latre et al. used the default settings for CSMA algorithm and estimated the maximum throughput as 148.8 kb/s and 162.2 kb/s for acknowledged and unacknowledged single-hop transmission, respectively. Choi and Zhou optimized the CSMA algorithm parameters in their work [7] and reported an increase in the estimation for the maximum throughput up to 167.6 kb/s and 189.5 kb/s for acknowledged and unacknowledged transmission, respectively (calculated using the equations provided in [7] for the 116 bytes of the medium access control (MAC) payload).

Performance of the IEEE 802.15.4 beacon-enabled mode is discussed e.g., in [3,8,13]. Although [3] and [13] introduce the basic models that can be used for analysing the maximum throughput in the CAP of the IEEE 802.15.4, no actual results revealing the maximum throughput are presented in these papers. Similarly, [8] provides the general framework for analysing data transmission during the CFP, but no actual values of the maximum throughput are reported.

In [5] and [16], performance of the IEEE 802.15.4 for specific scenarios with high throughput requirements, namely the streaming of audio data [5] and the transmission of electrocardiogram (ECG) measurements [16], was studied. In [5], Brunelli et al. analysed the feasibility of using ZigBee-based networks for low-rate streaming. The results presented in [5] reveal that under some pre-conditions, the maximum throughput over ZigBee networks is unaffected by the number of hops and reaches 30 kbps, which is sufficient for some voice streaming applications. In [16], Liang and Balasingham studied the performance of an ECG monitoring system based on IEEE 802.15.4. The results of the transmission delay, end-to-end latency and packet delivery rate analyses were presented.

An interesting conclusion was driven by the authors in [26]. In their research, Suh, Mir and Ko [26] propose an enhancement to IEEE 802.15.4 that adaptively adjusts the active period based on the traffic. Based on obtained results, the authors in [26] conclude that the IEEE 802.15.4 beacon-enabled mode is less effective than the nonbeacon-enabled mode for high-traffic applications.

Thus, although multiple papers have discussed IEEE 802.15.4 maximum throughput, none provide a comprehensive picture. Additionally, the existing analyses are often based on differing assumptions about data frame formats (e.g., different lengths of address fields) and use different values for the variable parameters of the standard mechanisms (e.g., CSMA), which complicates the comparison of the results.

## 3. IEEE 802.15.4 standard

The initial version of the IEEE 802.15.4 standard was introduced in 2003 under the name IEEE 802.15.4-2003 [29]. In 2006 and 2011, two revisions to the standard namely the IEEE 802.15.4-2006 [30] and IEEE 802.15.4-2011 [32], were introduced. The standard [32] defines the physical (PHY) layer and MAC sublayer for enabling low complexity, low power consumption and low data rate wireless connectivity among inexpensive devices. IEEE 802.15.4 was used as the basis for the various upper-layer standards e.g., ZigBee [33], 6LoWPAN [22], WirelessHART [31] and ISA100.11a [33].

The most recent revision of IEEE 802.15.4 ([32]) defines 12 possible options for PHY. Table 1 summarizes the IEEE 802.15.4-2011 PHY options that can be used within the license-free industrial, scientific and medical (ISM) band. Of these, the 2450 DSSS is the most widely used option today [1]. Thus, we will consider this PHY, unless stated otherwise.

The standard [32] supports two types of personal area networks (PAN). The first type is the beacon-enabled PANs, which contain the PAN coordinator node that periodically transmits beacon frames. The beacon frames bound the superframes and are used to synchronize all devices within PAN. The beacon frames contain data that identify the PAN and describe the superframe structure used [32]. As revealed in Fig. 1, the superframes can include active and inactive portions. It is expected that there is no communication during the inactive period. Thus, the nodes can switch to low-power sleep mode to save energy. The active period is divided into 16 slots with equal duration that form the CAP and, optionally, the CFP. The beacon interval (BI) and the superframe duration (SD) are defined in [32] as (1) and (2) respectively. In (1) and (2), *SO* and *BO* are the superframe and the beacon orders, respectively.

$$BI = aBaseSuperframeDuration \cdot 2^{BO} \quad (1)$$

$$SD = aBaseSuperframeDuration \cdot 2^{SO} \quad (2)$$

In (1) and (2), *aBaseSuperframeDuration* is a constant equal to 960 symbols (i.e., 15.36ms for 2450 DSSS PHY – see Table 1) and $0 \leq SO \leq BO \leq 14$. The *BI* and *SD* for IEEE 802.15.4 2450 DSSS can have values ranging from 15.36ms to 251.66s. The CAP starts immediately after the beacon and should last at least *aMinCAPLength* symbols (i.e., 440, as defined in [32]) under normal conditions. Therefore, the minimum length of the CAP period

for the 2450 DSSS PHY is equal to 7ms. If used, the CFP starts on the slot boundary immediately following the CAP and ends before the end of the active portion of the superframe [32]. The CFP can include up to seven guaranteed time slots (GTSs) that are assigned by the network coordinator and should "be used only for communications between the PAN coordinator and a device associated with the PAN through the PAN coordinator" [32]. The GTS can occupy more than one slot period [32] (see Fig. 1).

The second type of networks supported by the IEEE 802.15.4 is nonbeacon-enabled ones. Although the beacon frames in a nonbeacon-enabled network can be used (e.g., to support the network discovery), the superframes in those networks are not used.

IEEE 802.15.4-2011 defines two types of channel access mechanisms to be used for different networks [32]. The nonbeacon-enabled PANs use the unslotted Carrier Sense Multiple Access with Collision Avoidance (CSMA-CA) algorithm. The beacon-enabled PANs use the slotted CSMA-CA mechanism for transmitting data and command frames within the CAP. For transmitting the beacons and acknowledgement (ACK) frames, and for transmission in CFP, the CSMA-CA is not used. The CSMA-CA algorithm, as specified in [32], is presented in Fig. 2.

To give the receiver sufficient time for received frame processing, the standard [32] prescribes that two successive frames transmitted by a device must be separated by at least an IFS period. The length of the IFS after the frame transmission depends on the size of the frame. For a 2450 DSSS, the frame with a MAC protocol data unit (MPDU) of less than 19 bytes should be followed by a short IFS (SIFS), which is equal to 12 symbols [32]. Longer frames must be followed by the long IFS (LIFS) of 40 symbols. In the case of acknowledged frame transmission, the IFS starts after the reception of the ACK frame [32].

IEEE 802.15.4 [32] defines four possible types of frames: beacon, data, ACK and MAC command. The general format of frames prescribed by IEEE 802.15.4 for 2450 DSSS PHY is illustrated in Fig. 3. Each frame starts with the synchronization header (SHR) that is used for bit- and byte-wise synchronization. The PHY header (PHR) is used to specify the length of the PHY payload (i.e., MPDU). The MAC header (MHR) stores the required information about the frame type, format of different fields and other features, and it contains the sequence identifier of the frame. The MHR contains the addressing data, which depend on the frame type [32]. For example, ACK frames do not have any address data. The length of the addressing data field for a data frame can be between 4 and 20 bytes. For our research, we suppose that the length of the address data is six bytes (two bytes for each: source address, destination address and destination PAN ID). The maximum size of the MAC payload (MAC service data unit - MSDU) varies for different frame types. For data frames, the maximum length of MPDU is 116 bytes. The last two bytes of the MPDU contain the 16-bit ITU-T cyclic redundancy check (CRC) that is calculated over the MHR and MAC payload fields [32].

IEEE 802.15.4 PAN can contain up to three different types of nodes. The first is the PAN coordinator. The PAN coordinator is the primary controller of PAN [32], and in IEEE 802.15.4, PAN can have only a single PAN coordinator. The second type of nodes are the coordinators that provide the synchronization services for other devices [32]. The last type of nodes are leaf nodes that can communicate with coordinators and have no associated nodes [32].

## 4. Analysis of the maximum data streaming throughput in IEEE 802.15.4 PAN

### *4.1 Problem statement*

The topology of the network that we have targeted in our research is depicted in Fig. 4. We assume that an *infinite* block of data must be transmitted from node $k$ to node 0 over $k$ hops. We suppose that each node in PAN is equipped with a single transceiver working

according to the IEEE 802.15.4 specification [32]. At any moment, the transceiver can be in one of the three states: receive, transmit or sleep.

We denote the distance between nodes *i* and *i+1* as $R_{i,i+1}$. Additionally, we assume that the maximum transmission range, under which we understand the range within which a transmitted frame can be successfully received [4], for each node in the chain is equal to $R_{TX}$. Therefore, $\forall i \in [0, k-1]\ R_{i,i+1} \leq R_{TX}$. Additionally, we specify the interference range, $R_{INT}$, under which we understand the range within which the stations will suffer losses due to the interference from the transmission by this node [4]. Additionally, we designate the carrier sensing range, $R_{CS}$, within which the other nodes can detect a transmission by this node. As has been shown in [4], for the real-life systems $R_{TX}<R_{INT}<R_{CS}$ and in our further analysis, we will imply this relation.

Additionally, we assume that the preparation of each data frame before the transmission requires $T_{TXprep}$ seconds. The cumulative time for transferring each received frame between the MAC and the upper layers and data processing by the upper layers of the PAN coordinator is $T_{RXproc}$ seconds.

Our target is to define the maximum throughput for the MAC-layer user data obtainable for beacon-enabled and nonbeacon-enabled IEEE 802.15.4 PANs by implementing 2450 DSSS PHY.

### *4.2 Single-hop data transmission*

#### *4.2.1 Single-hop data transmission in beacon-enabled PAN*

In the case that the PAN coordinator decides to use the beacon-enabled mode, data transmission can be implemented either using only the CAP or using both the CAP and the CFP. Both scenarios are discussed below.

##### *4.2.1.1 Data transmission in CAP*

The phases for a data frame transmission in CAP in an IEEE 802.15.4 beacon-enabled PAN are depicted in Figs. 5a and 5b for acknowledged and unacknowledged frame transmission, respectively. The lengths of the phases for 2450 DSSS PHY, according to the standard [32], are summarized in Table 2. Note, that phases 1+2+3+4+5+6 and phase E, as well as phases 10+11+12+13+τ+E and phase P can overlap. The minimum periods for successive acknowledged and unacknowledged transmissions of a data frame with n-byte ($0 \leq n \leq 116$) MAC payload in CAP are defined as (3) and (4) respectively.

$$\mathrm{T_{CAPpktACK}}(N, \mathrm{T_{TXprep}}, \mathrm{T_{RXproc}}, \tau, \mathrm{T}_{rand}) = \left\lceil \left( \max\left(\tau + \mathrm{T_{ACK}} + \max(\mathrm{T_{IFS}}(n); \mathrm{T_{TXprep}}(n) + \max(\mathrm{T_{swRX}}; \mathrm{T}_{rand}) + \mathrm{T_{CCA1}} + \mathrm{T_{CCA2}} + \mathrm{T_{swTX}}); \mathrm{T_{RXproc}}(n)\right) + \tau + \mathrm{T_{Datapkt}}(n)\right) / \mathrm{T_{BO}} \right\rceil \cdot \mathrm{T_{BO}} = \left\lceil \left( \max\left(\tau + 0.544ms + \max\left(\mathrm{T_{TXprep}}(n) + 0.832ms; \mathrm{T_{RXproc}}(n)\right)\right) + \tau + 0.544ms + \frac{n \cdot 8}{250}\right) / 0.32ms \right\rceil \cdot 0.32ms \quad (3)$$

$$\mathrm{T_{CAPpktNACK}}(N, \mathrm{T_{TXprep}}, \mathrm{T_{RXproc}}, \tau, \mathrm{T}_{rand}) = \left\lceil \left( \max(\mathrm{T_{IFS}}(n); \mathrm{T_{TXprep}}(n) + \max(\mathrm{T_{swRX}}, \mathrm{T}_{rand}) + \mathrm{T_{CCA1}} + \mathrm{T_{CCA2}} + \mathrm{T_{swTX}}; \mathrm{T_{RXproc}}(n) + \tau) + \mathrm{T_{Datapkt}}(n)\right) / \mathrm{T_{BO}} \right\rceil \cdot \mathrm{T_{BO}} = \left\lceil \left( \max(\mathrm{T_{TXprep}}(n) + 832ms; \mathrm{T_{RXproc}}(n) + \tau) + 0.544ms + \frac{n \cdot 8}{250}\right) / 0.32ms \right\rceil \cdot 0.32ms \quad (4)$$

In (3) and (4), $\lceil x \rceil$ denotes the function that rounds *x* to the nearest integer greater than or equal to *x*. In (3) and (4), τ stands for the radio signal propagation delay. $\mathrm{T_{ACK}}$ and $\mathrm{T_{Datapkt}}(n)$ are defined via (5) and (6) respectively (see Table 2 for the duration of the phases for 2450 DSSS PHY).

$$\mathrm{T_{ACK}} = \mathrm{T_{ACKdelay}} + \mathrm{T_{TXhdr(A)}} + \mathrm{T_{TXdata(A)}} + \mathrm{T_{TXftr(A)}} = 0.544\ ms \quad (5)$$

$$\mathrm{T_{Datapkt}}(n) = \mathrm{T_{TXhdr(D)}} + \mathrm{T_{TXdata(D)}}(n) + \mathrm{T_{TXftr(D)}} = 0.544\ ms + \frac{n \cdot 8}{250} ms \quad (6)$$

Notation $max(a; b)$ denotes the function that returns $a$ if $a \geq b$ and $b$ if$a < b$. In addition, we assume in (3) and (4) that the minimum backoff exponent parameter (*macMinBE*) used by the CSMA-CA algorithm is equal to zero (therefore,$\mathrm{T}_{rand} = 0$). In

practice, this means that the collision avoidance is disabled during the first phase of CSMA-CA operation [32]. The same assumption we will use for our further analysis.

The effect of the frame size on the maximum throughput for error-less communication calculated using (3), (4) and (7) is depicted in Fig. 6. Fig.6 also illustrates the effect of the $T_{TXprep}$ and $T_{RXproc}$ for the cases when $T_{RXproc} = T_{TXprep} = 0$, $T_{RXproc} = T_{TXprep} = 2\,ms$ and when $T_{TXprep}$ and $T_{RXproc}$ are proportional to the number of transmitted bytes. This corresponds to the case when the IEEE 802.15.4 transceiver is connected to the microcontroller with a 115.2 kbit/s or 9.6 kbit/s UART interface (see, e.g. [19]).

$$Throughput\ (in\ kbit/s) = \frac{n \cdot 8}{T_{CAPpkt}(n, T_{TXprep}, T_{RXproc}, \tau)} \quad (7)$$

The edged shape of the curves in Fig. 6 is caused by the alignment of the data frame transmission start to the backoff period boundaries (the duration of the backoff period $T_{BO}$ is equal to 20 symbols, which is the duration of 10 data bytes) prescribed by [32] during CAP (consider Fig. 2). The blue line illustrates how the maximum throughput curve would look like, if not the transmission start alignment. As is possible to see in Fig. 6, the maximum throughput reaches 162 kbit/s for acknowledged and 181 kbit/s for unacknowledged data transfer in CAP. In addition, the presented results reveal that although the higher payloads generally give higher throughput, the use of the maximum payload does not guarantee the maximum throughput (see, e.g., curve for $T_{prep}$=2 ms without acknowledgement).

*4.2.1.2 Data transmission in CFP*

The second option for data transfer in beacon-enabled PAN is to use the CFP, which enables the devices to transmit without using the CSMA-CA mechanism. Once the GTSs in CFP are allocated, the transmission of data frames during the CFP will include the phases depicted in Figs. 5c and 5d. The lengths of the phases are summarized in Table 2. Note that for the unacknowledged data streaming scenario phases 1+2, τ+P and phase E can overlap. Similarly, for an acknowledged transmission, phases P, 6+7+8+9+τ+1+2 and 6+7+8+9+τ+E may overlap.

For the single-hop scenario, the minimum period between the transmissions of the successive data frames can be described as (8) and (9)

$$T_{CFPpktACK\_DSSS}(n, T_{TXprep}, T_{RXproc}, \tau) =$$
$$\max\left(\tau + T_{ACK} + \max\left(T_{IFS}(n); T_{TXprep}(n) + T_{swTX}\right); T_{RXproc}(n)\right) + \tau + T_{Datapkt}(n) =$$
$$\begin{cases} \max\left(\tau + 0.736ms + T_{TXprep}(n); T_{RXproc}(n)\right) + \frac{n \cdot 8}{250} + 0.544ms + \tau, n < 8\ bytes \\ \max\left(\tau + 0.544ms + max\left(T_{TXprep}(n) + 0.192ms; 0.64ms\right), T_{RXproc}\right) + \frac{n \cdot 8}{250} + 0.544ms + \tau, n \geq 8\ bytes \end{cases} \quad (8)$$

$$T_{CFPpktNACK\_DSSS}(n, T_{TXprep}, T_{RXproc}, \tau) = \max\left(T_{TXprep}(n) + T_{swTX}; T_{IFS}(n); \tau + T_{RXproc}(n)\right) +$$
$$T_{Datapkt}(n) = \begin{cases} \max\left(T_{TXprep} + 0.192ms, T_{RXproc} + \tau\right) + \frac{N \cdot 8}{250} + 0.544ms, n < 8\ bytes \\ \max\left(T_{TXprep} + 0.192ms, 0.64ms, T_{RXproc} + \tau\right) + \frac{N \cdot 8}{250} + 0.544ms, n \geq 8\ bytes \end{cases} \quad (9)$$

The curves illustrating the maximum throughput in CFP are presented in Fig. 7, which reveals that the maximum throughput in CFP reaches 170.6 kbit/s for acknowledged and 189.5 kbit/s for unacknowledged data transmission. The noticeable decline of throughput when increasing the payload from 7 to 8 bytes is caused by the change of the IFS from SIFS to LIFS (see Section 3).

*4.2.1.3 The maximum single-hop unidirectional data streaming throughput in an IEEE 802.15.4 beacon-enabled network*

In Sections 4.2.1.1 and 4.2.1.2, we have discussed the maximum throughputs possible for the errorless single-hop data transfer in CAP and CFP of an IEEE 802.15.4

beacon-enabled network. The presented results reveal that once the CFP is configured, the transmission in CFP enables higher throughput than CAP. The major reason for this is the absence of the CSMA-CS mechanism for data transfer in CFP.

The throughput for the single-hop connection over the IEEE 802.15.4 beacon-enabled network with both CAP and CFP phases in the case when the slot is much longer than the time required to send a single frame (i.e., $\frac{SD}{16} \gg T_{Datapkt}$) can be expressed as (10).

$$Throughput_{BE} = Throughput_{BE_{CAP}} \cdot \frac{T_{CAP}}{SD} + Throughput_{BE_{CFP}} \cdot \frac{T_{CFP}}{SD} = Throughput_{BE_{CAP}} \cdot \frac{SD \cdot \frac{N_{CAP}}{16} - T_{Beacon}}{SD} + Throughput_{BE_{CFP}} \cdot \frac{N_{CFP}}{16} \quad (10)$$

In (10), $Throughput_{BE_{CAP}}$ and $Throughput_{BE_{CFP}}$ stand for the throughput during the CAP and CFP, respectively; $T_{CAP}$ and $T_{CFP}$ are the durations of the CAP and CFP, while $T_{Beacon}$ is the duration of the beacon frame. The superframe duration is represented by SD, and $N_{CAP}$ and $N_{CFP}$ are the numbers of slots in CAP and CFP, respectively. As discussed in Section 3, the IEEE 802.15.4 standard prescribes having a minimum length of CAP equal to *aMinCAPLength*, and the CFP starts on the next slot boundary after the CAP. This can be specified as (11). For 2450 DSSS PHY, $T_{symbol}$ is equal to 16 $\mu s$ [32].

$$SD \cdot \frac{N_{CAP}}{16} > 440 \cdot T_{symbol} \quad (11)$$

It is easy to see that the throughput (10) is the maximum and (11) is fulfilled in the case of the longest possible SD, $N_{CAP}$=1 and $N_{CFP}$=15. The case calculated using (10) with maximum throughput in the IEEE 802.15.4 beacon-enabled network if $T_{Beacon}$=0.736 ms (i.e., the beacon has superframe specification data and data for a single GTS, but no beacon payload) is presented in Table 3.

*4.2.2 Single-hop data transmission in nonbeacon-enabled PAN*

Data transmission in nonbeacon-enabled IEEE 802.15.4 is executed using the unslotted version of the CSMA-CA mechanism (see Fig. 2). The main phases for acknowledged and unacknowledged data frame transfer over nonbeacon-enabled networks are illustrated in Figs. 5e and 5f. The durations of the phases can be found in Table 2. The minimum period for acknowledged and non-acknowledged frame transmission for single-hop unidirectional data streaming in an IEEE 802.15.4 nonbeacon-enabled network can be expressed as (12) and (13), respectively. The chart illustrating the effect of payload size on the maximum throughput in nonbeacon-enabled PAN is presented in Fig. 8.

$$T_{NBEpktACK}(N, T_{TXprep}, T_{RXproc}, \tau, T_{rand}) = \max\left(\tau + T_{ACK} + \max(T_{IFS}(n); T_{TXprep}(n) + \max(T_{swRX}; T_{rand}) + T_{CCA} + T_{swTX}); T_{RXproc}(n)\right) + \tau + T_{Datapkt}(n) = \begin{cases} \max\left(\tau + 1.056ms + T_{TXprep}(n); T_{RXproc}(n)\right) + \tau + \frac{N \cdot 8}{250} + 0.544ms, n < 8\ bytes \\ \max\left(\tau + 0.544ms + \max(0.64\ ms; T_{TXprep}(n) + 0.512ms); T_{RXproc}(n)\right) + \tau + \frac{N \cdot 8}{250} + 0.544ms, n \geq 8\ bytes \end{cases} \quad (12)$$

$$T_{NBEpktNACK}(N, T_{TXprep}, T_{RXproc}, \tau, T_{rand}) = \max\left(T_{IFS}(n); T_{TXprep}(n) + \max(T_{swRX}; T_{rand}) + T_{CCA} + T_{swTX}; \tau + T_{RXproc}(n)\right) + T_{Datapkt}(n) = \begin{cases} \max\left(T_{TXprep}(n) + 0.512ms; \tau + T_{RXproc}(n)\right) + \frac{N \cdot 8}{250} + 0.544ms, n < 8\ bytes \\ \max\left(0.64ms; T_{TXprep}(n) + 0.512\text{ms}; \tau + T_{RXproc}(n)\right) + \frac{N \cdot 8}{250} + 0.544ms, n \geq 8\ bytes \end{cases} \quad (13)$$

The values of the maximum throughput in IEEE 802.15.4 nonbeacon-enabled PAN for acknowledged and unacknowledged transmission are presented in Table 3. As revealed in Table 3 and Figs. 6 and 8, the maximum throughput for the single-hop data streaming in the nonbeacon-enabled PAN is higher than in the CAP of a beacon-enabled PAN. The major reasons for this are the alignment of the transmission to the backoff period boundary

and the longer channel testing phase (refer to Fig. 2) in the CAP of the beacon-enabled PAN prescribed by the standard [32].

As revealed in Table 3, if not accounting for the time for frame preparation and data processing, the maximum throughput of the beacon-enabled IEEE 802.15.4 PAN with 2450 DSSS PHY is slightly lower than the nonbeacon-enabled PAN. This result might seem unbelievable at first, but it can be understood by considering that the channel check using the CSMA/CA algorithm and other service operations can be executed during the IFS period. With this consideration, it becomes obvious that the maximum throughput for nonbeacon-enabled PAN and during CFP in beacon-enabled PAN is equal. Meanwhile, the beacon-enabled network requires some extra time to send the beacon and should have a CAP lasting at least 1/16 of the active period (see Section 3). As shown in Section 4.2.1.2, the longer phase for channel testing and the alignment of the transmission's start to the backoff period's boundaries results in lower throughput in the beacon-enabled PAN during the CAP than during the CFP.

Nonetheless, for high $T_{TXprep}$, the beacon-enabled PAN has higher maximum throughput than the nonbeacon-enabled PAN, although the difference is insignificant.

### *4.3 Multi-hop scenario*

The generic scenario for the wireless multi-hop unidirectional unacknowledged data transmission and its throughput were studied by Mao in [17]. In [17], the author found that for the case when $\forall i \in [0, k-1]\, R_{i,i+1} = R_{TX} = 0.5 \cdot R_{INT}$, the maximum unidirectional data transmission throughput over *k* hops is equal to one-third of the maximum single-hop transmission throughput. Similar results were obtained by Guo and Little and presented in [9,10]. Additionally, Theorem 3 in [17] states that in an error-free environment, a *k*-hop path where all links have a capacity equal to 1 can achieve the maximum throughput of $1/\omega(G)$ or equivalently $1/(\gamma(G)+1)$, where *G* is the conflict graph of the path, $\omega(G)$ is the clique number of the conflict graph *G* and $\gamma(G)$ is the maximum forward degree of the conflict graph *G*. The physical meaning of $\gamma(G)$ refers to the maximum number of nodes located between any node and the final receiver that are affected by this node's transmission. In his work, Mao [17] showed that maximum throughput can be achieved by dividing all the links into $\omega(G)$ independent sets and scheduling each set of links to be active for the same amount of time. In Sections 4.3.1 and 4.3.2, we will use these results and the previously obtained single-hop transmission throughput estimations to estimate the maximum throughput for multi-hop data transmission.

#### *4.3.1 Multi-hop data transmission in beacon-enabled PAN*

To enable multi-hop data transfer in IEEE 802.15.4 beacon-enabled PAN, the standard [32] prescribes each coordinator that is not the PAN coordinator to maintain the timing for both the incoming (i.e., the one transmitted by the upper-layer coordinator) and outgoing (i.e., the one transmitted by the coordinator itself) beacons. Naturally, the outgoing superframe must be completed during the inactive period of the incoming superframe. The relative timing of the superframes is defined using the *StartTime* parameter, as illustrated in Fig. 9. It is easy to see from (1) and (2) that the length of the BI for the beacon-enabled IEEE 802.15.4 is always equal to SD multiplied by the power of two (see (14)).

$$BI = SD \cdot 2^{BO-SO}\ ,\ 0 \le BO - SO \le 14 \qquad (14)$$

Meanwhile, as has been discussed in the previous section, the maximum throughput over *k*-hop links is determined by the clique number of its conflict graph $\omega(G) \in \{1,2,\dots k\}$, which is related to the number of conflicting nodes in the bottleneck segment. Therefore, for data transfer in the beacon-enabled PAN CFP, $\omega(G)$ can be presented as (15).

$$\omega_{BE}(G) = \gamma_{BE}(G) + 1 = \max_{i=0..k}\left|\left\{j\middle|(i \neq j)\wedge\left(R_{i,j} \leq R_{INT}\right)\right\}\right|, j = i..k \quad (15)$$

To obtain the maximum throughput, all the links in PAN should be divided into $\omega(G)$ independent sets that will be active for the same amount of time [17]. Therefore, for the beacon-enabled IEEE 802.15.4 PAN, the maximum throughput is equal to (16), where $\gamma(G) + 1$ is defined using (15) and $Throughput_{BE\_single\ hop}$ is the maximum single-hop throughput presented in Table 3.

$$Throughput_{k\ hops\_BE(best\ case)} = \frac{Throughput_{BE\_single\ hop}}{2^{\lceil \log_2(\gamma_{BE}(G)+1)\rceil}} \quad (16)$$

Note, that for the network presented in Fig. 2, we supposed that the carrier sensing range, $R_{CS}$, is higher than the interference range, $R_{INT}$. In that case, the total throughput could be slightly lower than (16) due to frames' collisions and unsuccessful media access attempts during CAP. In the worst case (i.e. when no data are transferred in CAP), the maximum throughput is equal to (17) (We assume that that $N_{CAP}$=1 and $N_{CFP}$=15, as in Section 4.2.1.3.). In (17), $Throughput_{CFP}$ stands for the maximum throughput during CFP (see Table 3).

$$Throughput_{k\ hops\_BE(worst\ case)} = \frac{15 \cdot Throughput_{CFP}}{16 \cdot 2^{\lceil \log_2(\gamma_{BE}(G)+1)\rceil}} \quad (17)$$

The chart illustrating the throughput over the beacon-enabled multi-hop IEEE 802.15.4 PAN with 2450 DSSS PHY for the best (16) and the worst-case (17) scenarios is depicted in Fig. 10. For the multi-hop data streaming scenario, as revealed in Fig. 10, when $\gamma(G) + 1 \neq 2^m, m \in \{0,1..\lfloor \log_2 k \rfloor\}$, the relation between BI and SD (14) imposed by the IEEE 802.15.4 standard [32] does not allow full utilization of the available channel resources.

*4.3.2 Multi-hop data transmission in nonbeacon-enabled PAN*

The multi-hop data transmission in the nonbeacon-enabled network is out of the scope of the IEEE 802.15.4 standard [32]. Using the same approach as in Section 4.3.1, we can define the maximum throughput for multi-hop data transmission as (21), where $\omega_{NBE}(G)$ is specified via (22) and $Throughput_{NBE\_single\ hop}$ is the maximum single-hop throughput that can be found in Table 3. The effect of $\gamma_{NBE}(G)$ on the maximum throughput is illustrated in Fig. 11.

$$Throughput_{k\ hops\_NBE} = \frac{Throughput_{NBE\_single\ hop}}{\gamma_{NBE}(G)+1} \quad (21)$$

$$\omega_{NBE}(G) = \gamma_{NBE}(G) + 1 = \max_{i=0..k}\left|\left\{j\middle|(i \neq j)\wedge\left(R_{i,j} \leq R_{CS}\right)\right\}\right|, j = i..k \quad (22)$$

As is possible to see from (15), for multi-hop data transfer in beacon-enabled PAN with CFP, the maximum possible throughput is defined by the maximum number of the nodes in the network located within the **interference range $R_{INT}$** (As during the CFP, carrier sensing is not used.). Meanwhile, as revealed in (22), the maximum multi-hop throughput for the nonbeacon-enabled PAN is defined by the maximum number of the nodes located in the **carrier sensing range $R_{CS}$**, which we assume to be higher than $R_{INT}$ [4]. Unfortunately, we are not aware of any experimental results that reveal the relation between the $R_{CS}$ and $R_{INT}$ for actual 802.15.4 transceivers. Therefore, we cannot define which of the networks (beacon-enabled or nonbeacon-enabled) is capable of providing higher throughput. Nonetheless, as can be seen in Figs. 10 and 11, if $R_{CS} \approx R_{INT}$ for $\gamma(G) + 1 = 2^m, m \in \boldsymbol{N}$, the maximum throughput in the beacon-enabled and nonbeacon-enabled scenarios is about the same. For the case of $\gamma(G) + 1 \neq 2^m, m \in \boldsymbol{N}$, the nonbeacon-enabled PAN has higher throughput than the beacon-enabled one.

## 5. Evaluation of the maximum data streaming throughput in IEEE 802.15.4 PANs

*5.1 Experiment set-up*

In Section 4, we analysed the IEEE 802.15.4 protocol and obtained estimations for the maximum possible throughput for the single-hop and the multi-hop data transfer in beacon-enabled and nonbeacon-enabled PANs. Nonetheless, other researchers in their experiments (e.g., [15,27]) and in the previous experiments using the CC2430 System-on-Chip (SoC) modules from Texas Instrument and the TIMAC protocol stack (see e.g., [18]), we were unable to obtain throughput exceeding 150 kbit/s. Therefore, we have decided to evaluate whether the contemporary IEEE 802.15.4 transceivers are capable of providing the high throughput values obtained during the analysis.

For our experiments, we used CC2530 SoC modules from Texas Instruments, which combine an IEEE 802.15.4 2450-DSSS compatible transceiver with an industry-standard enhanced 8051 microcontroller core [34]. The microcontroller has the maximum clock frequency of 32 MHz and contains up to 256 kB of flash memory and 8 kB of random-access memory (RAM). For the experiment, we developed embedded software that implemented data transfer according to the IEEE 802.15.4 for both beacon-enabled and nonbeacon-enabled modes. In the developed embedded software, we used the available hardware features of the transceiver to minimize the processing time. For example, the transmission of the ACK frames was executed by the transceiver automatically without any interference from the microcontroller core. Additionally, to execute the CSMA-CA algorithm, we used a command strobe/CSMA-CA processor (CSP) that is part of the transceiver. This allowed us to quicken the CSMA-CA execution while minimizing the load on the microcontroller core. Additionally, we optimized the process of data transfer between the microcontroller and the transceiver. The new data frame was loaded to the First In, First Out (FIFO) transmit buffer of the transceiver during the IFS, immediately after the successful transmission of the previous data frame (i.e., once the last data byte of the previous frame was sent over the radio interface in the case an unacknowledged frame transmission; once the ACK frame for the previously transmitted frame was received in the case of an acknowledged transmission).

In our experiments, we used six radio modules and evaluated the maximum throughput available for networks with one to five hops. During the experiments, the nodes were placed indoors at a distance of around half a meter from each other, and the transmission power for all nodes was set to 0dBm. Therefore, all the nodes were located within the interference and carrier-sense ranges of each other. Before the experiments, the used frequency channel was checked to confirm the absence of interference from other systems.

During the experiments, we controlled the amount of received and transmitted data, beacons and acknowledgement frames for each node. Additionally, we measured the total time required to send 1000 data frames over the network and the latency for data frame transfer, which was defined as the period from the start of data frame transmission at the first node to the reception of that frame by the last node. The measurement of the total transmission time and the latency was completed using an oscilloscope connected to the first and the last nodes in the chain.

The measurements were repeated for acknowledged and unacknowledged data transfer using the different operation modes with various numbers of hops in PAN, different MAC payload sizes, as well as differing SO and BO values. For the beacon-enabled PAN, the measurements were completed for two modes, superframe with only CAP ($N_{CAP}$=16, $N_{CFP}$=0) and superframe with both CAP and CFP ($N_{CAP}$=1, $N_{CFP}$=15). For the nonbeacon-enabled PAN, we made measurements using two different software versions. The first maximized the throughput, and the second minimized the latency. The difference between these versions is discussed in Section 5.2.

### *5.2 Evaluation of results*

The values for the maximum real-life throughput for the different numbers of hops are summarized in Table 4 and presented in Fig. 12. Comparison of the experimental results with the analytic results presented in Table 3 and in Figs. 10 and 11 reveals that the analytic values for the maximum throughput in the beacon-enabled PAN are close to the experimental ones. Meanwhile, for nonbeacon-enabled PAN with more than three nodes, the experimental throughput appears to be even higher than the analytic expectations. This occurs because the analytic result was obtained using the maximum throughput for the single-hop, which assumes an IFS delay between the successive frames transmitted by a node (see Section 4.2). Meanwhile, for the tested multi-hop transmission scenario, the IFS delay between the packets was not required, as successive data frames were always transmitted by different nodes. One of the consequences of this, which can easily be seen from the obtained results, is that multi-hop data transmission in the real-life nonbeacon-enabled PAN scenario appeared to be faster than in the beacon-enabled one.

The other reason for nonbeacon-enabled PAN having higher throughput is the effect of the data buffer overflow for beacon-enabled PANs. In our experiments in the nonbeacon-enabled PAN, a data frame received from node *i* was transmitted by node *i-1* either immediately (latency-optimized PAN) or after reception of the next data frame from node *i* (throughput-optimized PAN). In the first case, node *i-1* required some additional time before retransmitting the frame to copy data from the transceiver RX FIFO to the TX FIFO. Meanwhile, in the second case, once frame *n* was received, node *i-1* just issued the command to the transceiver to send the frame *n-1*, which *was* loaded into the TX FIFO of the transceiver in advance. This enabled us to increase the maximum throughput at the cost of decreased data transfer latency. The latency for data transfer over a five-hop network for the different modes is illustrated in Fig. 13.

Meanwhile, for the beacon-enabled PAN, during the whole superframe, the duration channel was used only by the single node (see Section 4.1.3 and Fig. 9). First, this required separating the data frames transmitted by a node during the superframe by the IFS. Additionally, it required node *i* to have a buffer to store data received from the upper-layer node (i.e., *i*+1) in the incoming superframe until they could be transmitted to the lower-layer node (i.e., *i*-1) during the outgoing superframe (consider Figs. 4 and 9). One of the related problems for actual systems is the potential for a data buffer overflow in the case of SO values becoming too high.

This effect of this can be clearly seen in Fig. 14, which shows the number of data frames transmitted by node four in a five-hop beacon-enabled PAN for different SO values. As revealed in Fig. 14, the number of transmitted data frames for SO=5 falls to 60-70% of the received frames. This occurs because of the effect of the data buffer overflow. CC2530 SoCs are equipped with 8 kB of RAM. Of this, 7090 bytes were utilized to store the received data. In the case of 116-byte data frame payloads, the buffer is capable of storing 61 data frames. Meanwhile, for example, the first node in the chain for unacknowledged data transmission and SO=5 (i.e., node five in a five-hop network) sends about 100 data frames in a single superframe. For the developed test software, the frames received once the buffer is filled are dropped. As can be seen in Fig. 12, the maximum throughput in a beacon-enabled PAN that uses only CAP is lower that the throughput in a beacon-enabled PAN with both CAP and CFP. This correlates with the analytic results presented in Section 4.2.

Fig. 13 reveals that the latency for data transfer in a nonbeacon-enabled network is typically lower than in a beacon-enabled PAN. In addition, the presented results reveal that the latency for the implemented latency-optimized nonbeacon-enabled PAN is significantly lower than in the throughput-optimized PAN. For the beacon-enabled PAN, the increase of the SO causes a linear increase of the data transfer latency.

The effects of the data frame payload and of the SO on the maximum throughput for the single-hop and five-hop data transfer scenarios are illustrated in Figs. 15 and 16. As can be seen, the maximum throughput for the single-hop scenario is obtained for the maximum payload and SO values, while for the multi-hop scenario, due to abovementioned features, the throughput is the highest when SO=4.

## 6. Conclusions

In this paper, we focus on the maximum throughput that can be obtained using the IEEE 802.15.4-based transceivers that operate in the license-free 2.4 GHz ISM band using the 2450 DSSS physical layer. The analytic information presented in the paper and the experimental results reveal that for single-hop data transfer, the maximum possible throughput for user MAC-level data is approximately 190 kbit/s for unacknowledged data transfer and 170 kbit/s for acknowledged data transfer. This throughput can be obtained both in beacon-enabled and in nonbeacon-enabled PANs. For data transfer over multiple hops in nonbeacon-enabled networks, the maximum throughput is inversely proportional to the highest forward degree of the network conflict graph, which is related to the maximum number of transfer chain nodes located within the carrier sense range. For the multi-hop transfer in the beacon-enabled network, the maximum throughput is inversely proportional to the next power of two of the maximum forward degree of the network conflict graph. For data transmission in CAP, the maximum forward degree depends on the number of transfer chain nodes located within the carrier sense range. Transmission using CFP is defined by the number of nodes within the interference range.

Note that this is the maximum possible throughput for IEEE 802.15.4 2450 DSSS compatible transceivers. The only possibility to increase the throughput further within the framework of IEEE 802.15.4 is to have multiple transceivers simultaneously employed for communication on different radio channels both on the transmitter and on the receiver nodes.

The results presented in this paper reveal that to obtain high throughput, one must use data frames with high payloads. Additionally, for single-hop transmission in beacon-enabled networks, one needs to use the highest possible values of SO and BO. For multi-hop data transmission, the SO and BO values that maximize the throughput depend on the maximum forward degree of the network conflict graph and the maximum size of the data buffers available on the nodes in the network. The presented results show that both for the multi-hop scenario in beacon-enabled and nonbeacon-enabled PANs, the operation modes that maximize throughput and minimize end-to-end latency differ.

Additionally, the results indicate that in the case when a transceiver is implemented as a standalone chip, data transfer between the transceiver and the central processor can limit the maximum achievable throughput. Therefore, for applications requiring high throughput, systems-on-chip, which combine the transceiver and the microcontroller core, are usually more efficient than the standalone solutions.

Although the results presented in the paper's analysis and evaluations were completed for the IEEE 802.15.4 protocol, we suppose that the obtained results can be used to improve the performance of the multiple protocols based on the IEEE 802.15.4, such as ZigBee [33], WirelessHART [31], ISA100.11a [33] or 6LoWPAN [22]. For the 6LoWPAN protocol, which enables transmission via Internet Protocol version 6 (IPv6) packets in IEEE 802.15.4 networks, the increase of the underlying 802.15.4 protocol's throughput is especially beneficial. As discussed in [11], the maximum 6LoWPAN application data payload in a single IEEE 802.15.4 frame is just 61 to 76 bytes. Therefore, to transfer data using 6LoWPAN, one has to send almost two times as many packets than when using the IEEE 802.15.4. In such a case, minimizing the period between sequential packets becomes especially important.

In the future, we will consider extending our analysis to account for erroneous environments, as well as determine the effects of relaxing some of the assumptions adopted for this paper.

**Acknowledgements**

The authors wish to thank Professor Kiseon Kim from Gwangju Institute of Science and Technology for valuable discussions and comments. We also wish to thank the Editor and anonymous reviewers for their valuable comments and suggestions.

This work was supported in part by European Regional Development Fund, Council of Oulu Region and Ylivieska Subregion.

**References**

[1] T. Aaberge, Low Complexity Antenna Diversity For IEEE 802.15.4 2.4 GHz PHY, M.Sc. Thesis, Norwegian University of Science and Technology, (2009).

[2] I. F. Akyildiz, T. Melodia and K. R. Chowdhury, A survey on wireless multimedia sensor networks, *Computer Networks* **51**(4) (2007), 921–960.

[3] A. N. Alvi, S. S. Naqvi, S. H. Bouk, N. Javaid, U. Qasim and Z. A. Khan, Evaluation of Slotted CSMA/CA of IEEE 802.15.4, in: *Procedings of 7th International Conference on Broadband, Wireless Computing, Communication and Applications (BWCCA)*, 2012, pp. 391–396.

[4] G. Anastasi, E. Borgia, M. Conti and E. Gregori, Wi-fi in ad hoc mode: a measurement study, in: *Procedings of Proceedings of the 2nd IEEE Annual Conference on Pervasive Computing and Communications (PerCom)*, 2004, pp. 145–154.

[5] D. Brunelli, M. Maggiorotti, L. Benini and F. L. Bellifemine, Analysis of Audio Streaming Capability of Zigbee Networks, in: *Wireless Sensor Networks*, R. Verdone,ed., Springer Berlin Heidelberg, 2008, pp. 189–204.

[6] A. Chlipala, J. Hui and G. Tolle, *Deluge: Data Dissemination for Network Reprogramming at Scale*, report, University of California at Berkeley, 2003.

[7] J. S. Choi and M. Zhou, Performance analysis of ZigBee-based body sensor networks, in: *Procedings of IEEE International Conference on Systems Man and Cybernetics (SMC)*, 2010, pp. 2427–2433.

[8] S. Fan, J. Li, H. Sun and R. Wang, Throughput analysis of GTS allocation in beacon enabled IEEE 802.15.4, in: *Procedings of 3rd IEEE International Conference on Computer Science and Information Technology (ICCSIT)*, 2010, pp. 561–565.

[9] S. Guo and T. D. C. Little, Throughput Estimation for Singleton Video Streaming Application over Wireless Sensor Network, in: *Procedings of 6th International Conference on Wireless Communications Networking and Mobile Computing (WiCOM)*, 2010, pp. 1–4.

[10] S. Guo and T. D. C. Little, QoS-enabled Video Streaming in Wireless Sensor Networks, in: *Procedings of 9th IEEE International Symposium on Network Computing and Applications (NCA)*, 2010, pp. 214–217.

[11] A. J. Jara, M. A. Zamora and F. Gomez-Skarmeta, Glowbal IP: An adaptive and transparent IPv6 integration in the Internet of Things, *Mobile Information Systems* **8**(3) (2012), 177–197.

[12] H. Jun, W. Zhao, M. H. Ammar, E. W. Zegura and C. Lee, Trading latency for energy in densely deployed wireless ad hoc networks using message ferrying, *Ad Hoc Networks* **5**(4) (2007), 444–461.

[13] M. Kohvakka, M. Kuorilehto, M. Hännikäinen and T. D. Hämäläinen, Performance analysis of IEEE 802.15.4 and ZigBee for large-scale wireless sensor network

applications, in: *Procedings of 3rd ACM International Workshop on Performance Evaluation of Wireless Ad Hoc, Sensor and Ubiquitous Networks (PE-WASUN)*, ACM, New York, NY, USA, 2006, pp. 48–57.

[14] B. Latré, B. Braem, I. Moerman, C. Blondia and P. Demeester, A survey on wireless body area networks, *Wireless Networks* **17**(1) (2011), 1–18.

[15] B. Latré, P. D. Mil, I. Moerman, B. Dhoedt, P. Demeester and N. V. Dierdonck, Throughput and Delay Analysis of Unslotted IEEE 802.15.4, *Journal of Networks* **1**(1) (2006).

[16] X. Liang and I. Balasingham, Performance analysis of the IEEE 802.15.4 based ECG monitoring network, in: *Procedings of 7th IASTED International Conference*, 2007, pp. 99–104.

[17] G. Mao, The Maximum Throughput of A Wireless Multi-Hop Path, *Mobile Networks and Applications* **16**(1) (2011), 46–57.

[18] K. Mikhaylov, N. Plevritakis and J. Tervonen, Analysis and Evaluation of Bluetooth Low Energy Performance, *Journal of Sensor and Actuator Networks* **submitted for publication** (2013).

[19] K. Mikhaylov and J. Tervonen, Evaluation of Power Efficiency for Digital Serial Interfaces of Microcontrollers, in: *Procedings of 5th International Conference on New Technologies, Mobility and Security (NTMS)*, 2012, pp. 1–5.

[20] K. Mikhaylov and J. Tervonen, Data Collection from Isolated Clusters in Wireless Sensor Networks Using Mobile Ferries, in: *Procedings of Advanced Information Networking and Applications Workshops (WAINA)*, 2013, pp. 903–909.

[21] S. Misra, M. Reisslein and G. Xue, A survey of multimedia streaming in wireless sensor networks, *IEEE Communications Surveys Tutorials* **10**(4) (2008), 18–39.

[22] G. Montenegro, N. Kushalnagar, J. Hui and D. Culler, IPv6 over IEEE 802.15.4, (2007).

[23] B. Nefzi and Y.-Q. Song, CoSenS: A collecting and sending burst scheme for performance improvement of IEEE 802.15.4, in: *Procedings of 35th IEEE Conference on Local Computer Networks (LCN)*, 2010, pp. 172–175.

[24] S. Soro and W. Heinzelman, A Survey of Visual Sensor Networks, *Advances in Multimedia* **2009** (2009), 21.

[25] T. Stathopoulos, J. Heidemann and D. Estrin, *A Remote Code Update Mechanism for Wireless Sensor Networks*, Technical Report, Center for Embedded Network Sensing, UC Los Angeles, 2003.

[26] C. Suh, Z. H. Mir and Y.-B. Ko, Design and implementation of enhanced IEEE 802.15.4 for supporting multimedia service in Wireless Sensor Networks, *Computer Networks* **52**(13) (2008), 2568–2581.

[27] T. Sun, L.-J. Chen, C.-C. Han, G. Yang and M. Gerla, Measuring effective capacity of IEEE 802.15.4 beaconless mode, in: *Procedings of IEEE Wireless Communications and Networking Conference (WCNC)*, 2006, pp. 493–498.

[28] M. Zhao and Y. Yang, Data Gathering in Wireless Sensor Networks with Multiple Mobile Collectors and SDMA Technique Sensor Networks, in: *Procedings of IEEE Wireless Communications and Networking Conference (WCNC)*, 2010, pp. 1–6.

[29] IEEE Standard for Information Technology - Telecommunications and Information Exchange Between Systems - Local and Metropolitan Area Networks Specific Requirements Part 15.4: Wireless Medium Access Control (MAC) and Physical Layer (PHY) Specifications for Low-Rate Wireless Personal Area Networks (LR-WPANs), *IEEE Std 802.15.4-2003* (2003), 1–670.

[30] IEEE Standard for Information Technology – Local and metropolitan area networks – Specific requirements – Part 15.4: Wireless Medium Access Control (MAC) and

Physical Layer (PHY) Specifications for Low Rate Wireless Personal Area Networks (WPANs), *IEEE Std 802.15.4-2006 (Revision of IEEE Std 802.15.4-2003)* (2006), 1–320.

[31] WirelessHART, *IEC 62591* (2010).

[32] IEEE Standard for Local and metropolitan area networks–Part 15.4: Low-Rate Wireless Personal Area Networks (LR-WPANs), *IEEE Std 802.15.4-2011 (Revision of IEEE Std 802.15.4-2006)* (2011), 1–314.

[33] Wireless systems for industrial automation: Process control and related applications, *ANSI/ISA-100.11a-2011* (2011).

[34] *A True System-on-Chip Solution for 2.4-GHz IEEE 802.15.4 and ZigBee Applications*, Texas Instruments, 2011.

Table 1: Main features of IEEE 802.15.4-2011 ISM band PHY options [32]

| PHY (MHz) | Frequency band (MHz) | Spreading parameters | | Data parameters | |
|---|---|---|---|---|---|
| | | Chip rate (kchip/s) | Modulation | Bit rate (kb/s) | Symbol rate (ksymbol/s) |
| 868/915 | 868-868.6 | 300 | BPSK | 20 | 20 |
| | 902-928 | 600 | BPSK | 40 | 40 |
| 868/915 (optional) | 868-868.6 | 400 | ASK | 250 | 12.5 |
| | 902-928 | 1600 | ASK | 250 | 50 |
| 868/915 (optional) | 868-868.6 | 400 | O-QPSK | 100 | 25 |
| | 902-928 | 1000 | O-QPSK | 250 | 62.5 |
| 2450 DSSS | 2400-2483.5 | 2000 | O-QPSK | 250 | 62.5 |
| 2450 CSSS (optional) | 2400-2483.5 | See [32] | CSSS + DQPSK | 250<br>1000 | 167 |

Table 2: Phase lengths for data frame transmission in IEEE 802.15.4 with 2450 DSSS [32]

| Transmission in CAP in beacon-enabled PAN | | Transmission in CFP in beacon-enabled PAN | | Transmission in nonbeacon-enabled PAN | | Phase duration, symbols | | Phase duration, ms | |
|---|---|---|---|---|---|---|---|---|---|
| Phase | Symbol | Phase | Symbol | Phase | Symbol | minimum | maximum | minimum | maximum |
| 1 | $T_{TXprep}$ | 1 | $T_{TXprep}$ | 1 | $T_{TXprep}$ | ND[1] | | ND[1] | |
| 2 | $T_{align}$ | | | | | 0 | 19 | 0 | 0.304 |
| 3 | $T_{rand}$ | | | 2 | $T_{rand}$ | 0[2] | 5100[3] | 0[2] | 81.63[3] |
| 4 | $T_{CCA1}$ | | | | | 20 | | 0.32 | |
| 5 | $T_{CCA2}$ | | | 3 | $T_{CCA}$ | 8 | | 0.128 | |
| 6 | $T_{swTX}$ | 2 | $T_{swTX}$ | 4 | $T_{swTX}$ | 12[4] | | 0.192[4] | |
| 7 | $T_{TXhdr(D)}$ | 3 | $T_{TXhdr(D)}$ | 5 | $T_{TXhdr(D)}$ | 30[5] | 58[6] | 0.48[5] | 0.928[6] |
| 8 | $T_{TXdata(D)}$ | 4 | $T_{TXdata(D)}$ | 6 | $T_{TXdata(D)}$ | 0 | 236 | 0 | 3.776 |
| 9 | $T_{TXftr(D)}$ | 5 | $T_{TXftr(D)}$ | 7 | $T_{TXftr(D)}$ | 4 | | 0.064 | |
| 10 | $T_{ACKdelay}$ | 6 | $T_{ACKdelay}$ | 8 | $T_{ACKdelay}$ | 12 | | 0.192 | |
| 11 | $T_{TXhdr(A)}$ | 7 | $T_{TXhdr(A)}$ | 9 | $T_{TXhdr(A)}$ | 18[7] | | 0.288[7] | |
| 12 | $T_{TXdata(A)}$ | 8 | $T_{TXdata(A)}$ | 10 | $T_{TXdata(A)}$ | 0 | | 0 | |
| 13 | $T_{TXftr(A)}$ | 9 | $T_{TXftr(A)}$ | 11 | $T_{TXftr(A)}$ | 4 | | 0.064 | |
| E | $T_{IFS}$ | E | $T_{IFS}$ | E | $T_{IFS}$ | 12[8]<br>40[9] | | 0.192[8]<br>0.64[9] | |
| τ | τ | τ | τ | τ | τ | ND | | ND | |
| P | $T_{RXproc}$ | P | $T_{RXproc}$ | P | $T_{RXproc}$ | ND[1] | | ND[1] | |

[1]- not defined in [32], depends on the transceiver hardware
[2] – Backoff exponent (BE) = 0
[3]– Backoff exponent (BE) = 8
[4]- [32] defines only RX-to-TX and TX-to-RX turnaround time
[5]- SHR (10 symbols) + PHR(2 symbols) + MHR(18 symbols) (see Fig. 3)
[6]- SHR (10 symbols) + PHR(2 symbols) + MHR(46 symbols) (see Fig. 3)
[7]- SHR (10 symbols) + PHR(2 symbols) + MHR(6 symbols) (see Fig. 3)
[8]- if MPDU size < 19 bytes
[9]- if MPDU size > 18 bytes

Table 3: Maximum throughput for beacon-enabled (BE) and nonbeacon-enabled (NBE) in single hop IEEE 802.15.4 PANs with 2450 DSSS PHY

| *Parameters* | *Maximum throughput, kbit/s(errorless scenario)* | | | | | | | |
|---|---|---|---|---|---|---|---|---|
| | *Acknowledged transmission* | | | | *Unacknowledged transmission* | | | |
| | BE CAP only | BE CFP only | **BE max** | **NBE** | BE CAP only | BE CFP only | **BE max** | **NBE** |
| $T_{RXproc} = T_{TXprep}$=0 | 170.6 | 161.8 | **170.0** | **170.6** | 189.5 | 181.3 | **189.0** | **189.5** |
| $T_{RXproc} = T_{TXprep} = 2ms$ | 132.7 | 120.8 | **132.0** | **126.9** | 143.9 | 129.5 | **143.0** | **137.1** |
| $T_{RXproc} = T_{TXprep} = \frac{10 \cdot n}{115.2}\ ms$ | 61.6 | 58.9 | **61.4** | **60.3** | 63.9 | 61.2 | **63.8** | **62.5** |
| $T_{RXproc} = T_{TXprep} = \frac{10 \cdot n}{9.6}\ ms$ | 7.4 | 7.3 | **7.4** | **7.4** | 7.4 | 7.4 | **7.4** | **7.4** |

Table 4: Experimental results for the maximum throughput in beacon-enabled (BE) and non-beacon-enabled (NBE) IEEE 802.15.4 PANs (maximum error: 5%)

| *Number of hops* | *Maximum throughput, kbit/s* | | | | | | | |
|---|---|---|---|---|---|---|---|---|
| | *Acknowledged transmission* | | | | *Unacknowledged transmission* | | | |
| | BE (CAP only) | BE (CAP + CFP) | NBE (latency) | NBE (throughput) | BE (CAP only) | BE (CAP + CFP) | NBE (latency) | NBE (throughput) |
| 1 | 160.6[1] | 169.0[1] | 170.6 | 170.6 | 180.4[1] | 191.1[1] | 190.2 | 190.2 |
| 2 | 79.3[2] | 82.9[2] | 49.9 | 89.2 | 87.5[2] | 91.9[2] | 95.5 | 98.4 |
| 3 | 38.3[3] | 38.7[3] | 39.5 | 57.5 | 44.2[3] | 45.9[3] | 62.7 | 64.7 |
| 4 | 38.0[3] | 39.7[3] | 32.0 | 43.4 | 43.4[3] | 45.5[3] | 46.4 | 47.7 |
| 5 | 20.0[4] | 21.0[4] | 27.3 | 34.7 | 21.8[4] | 22.7[4] | 37.1 | 37.9 |

[1]- BO=8, SO=8
[2]- BO=5, SO=4
[3]- BO=6, SO=4
[4]- BO=7, SO=4

Fig. 1. IEEE 802.15.4 superframe structure [32]

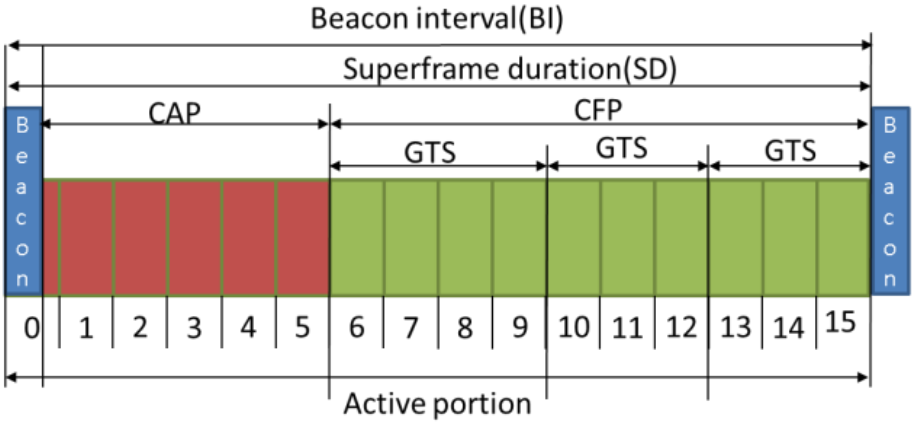


a) Example of a superframe without inactive period (i.e., SO=BO)

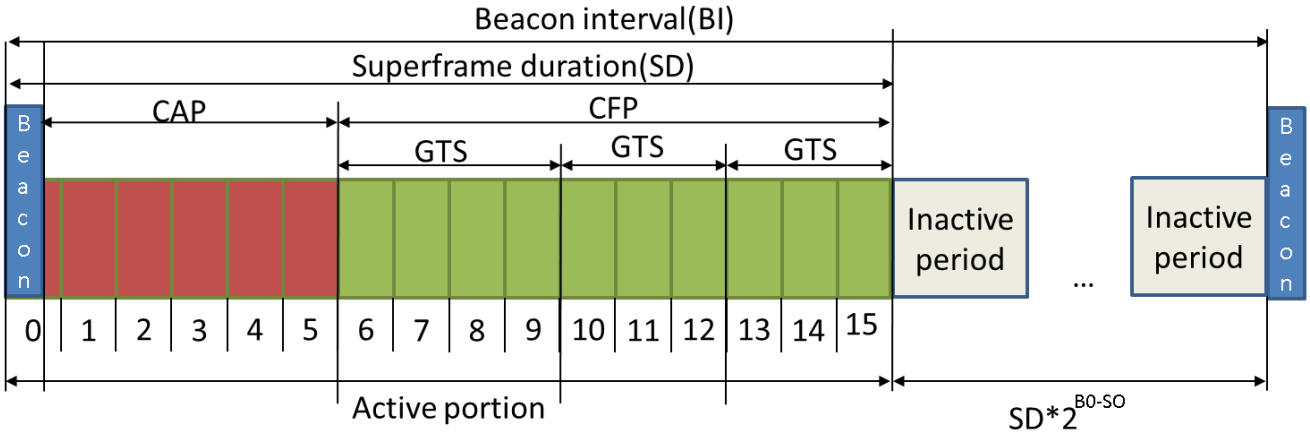


b) Example of a superframe with inactive period (i.e., SO<BO)

Fig. 2. IEEE 802.15.4 CSMA-CA algorithm [32] (for 2450 DSSS PHY: $0 \leq macMinBE \leq 8$ depending on the used settings [default value = 3]; $CW_0=2$; $0 \leq macMaxCSMABackoffs \leq 5$ [default value = 4])

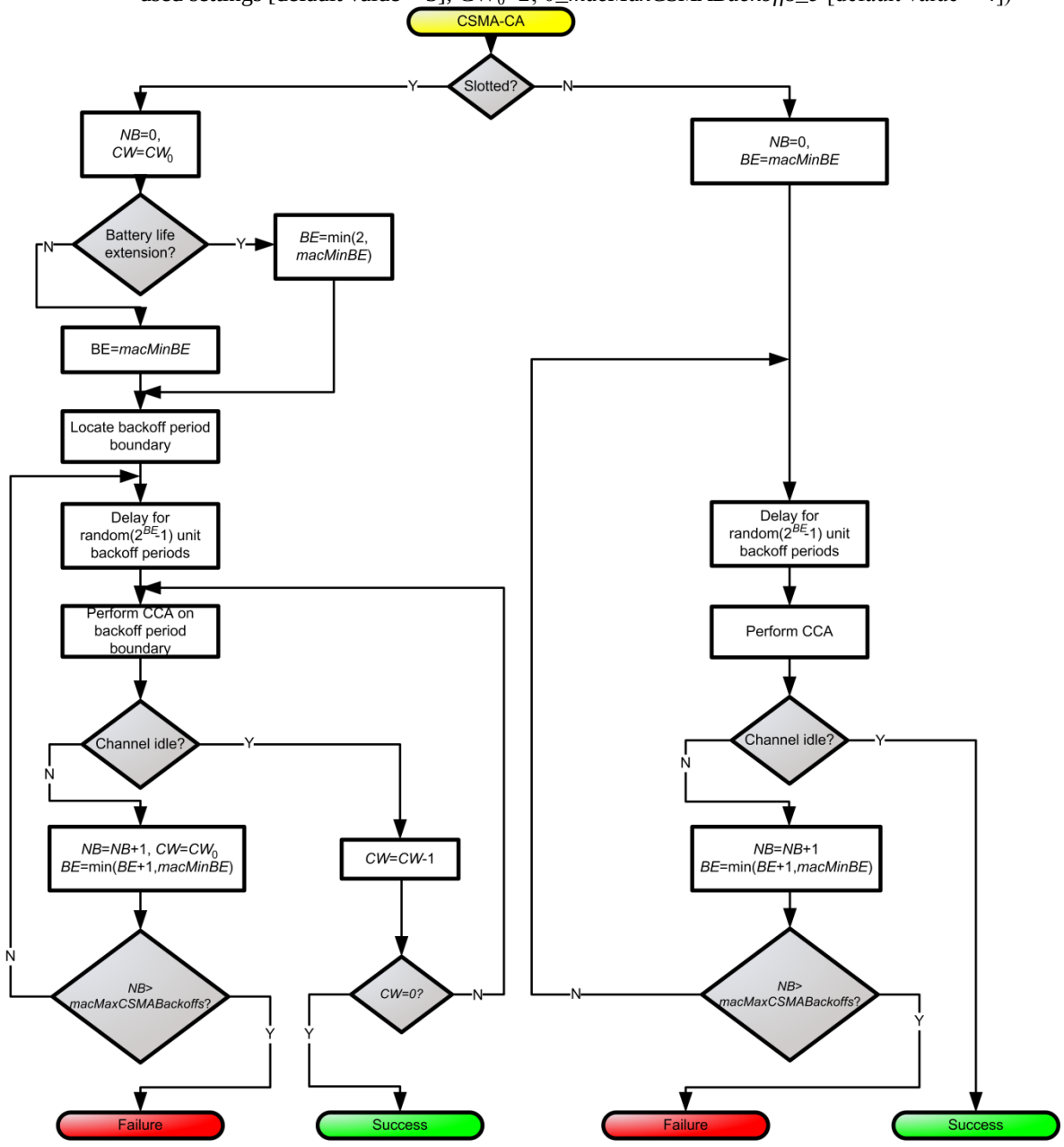

Fig. 3 IEEE 802.15.4 2450 DSSS frame format [32]
(security disabled)

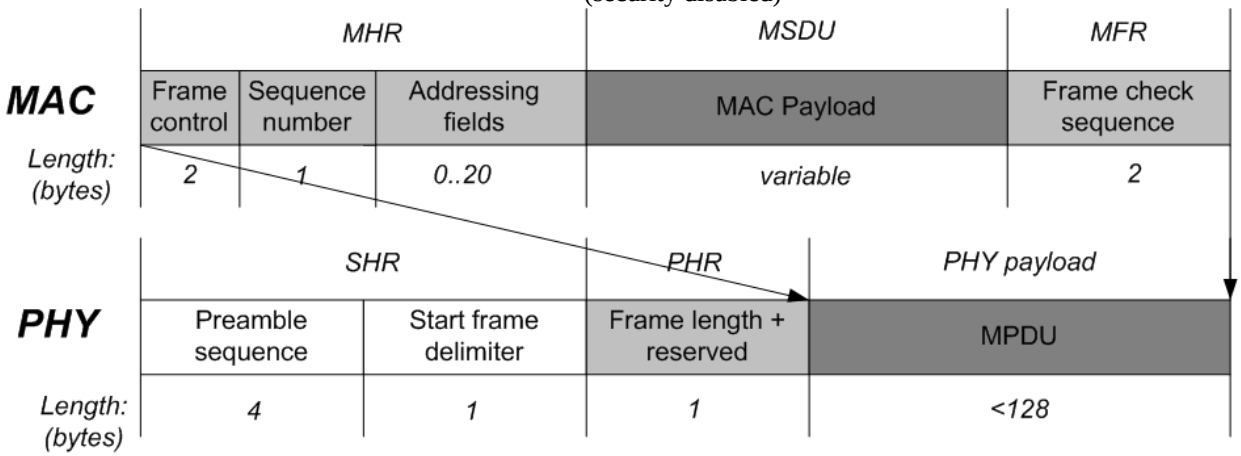


Fig. 4. PAN topology

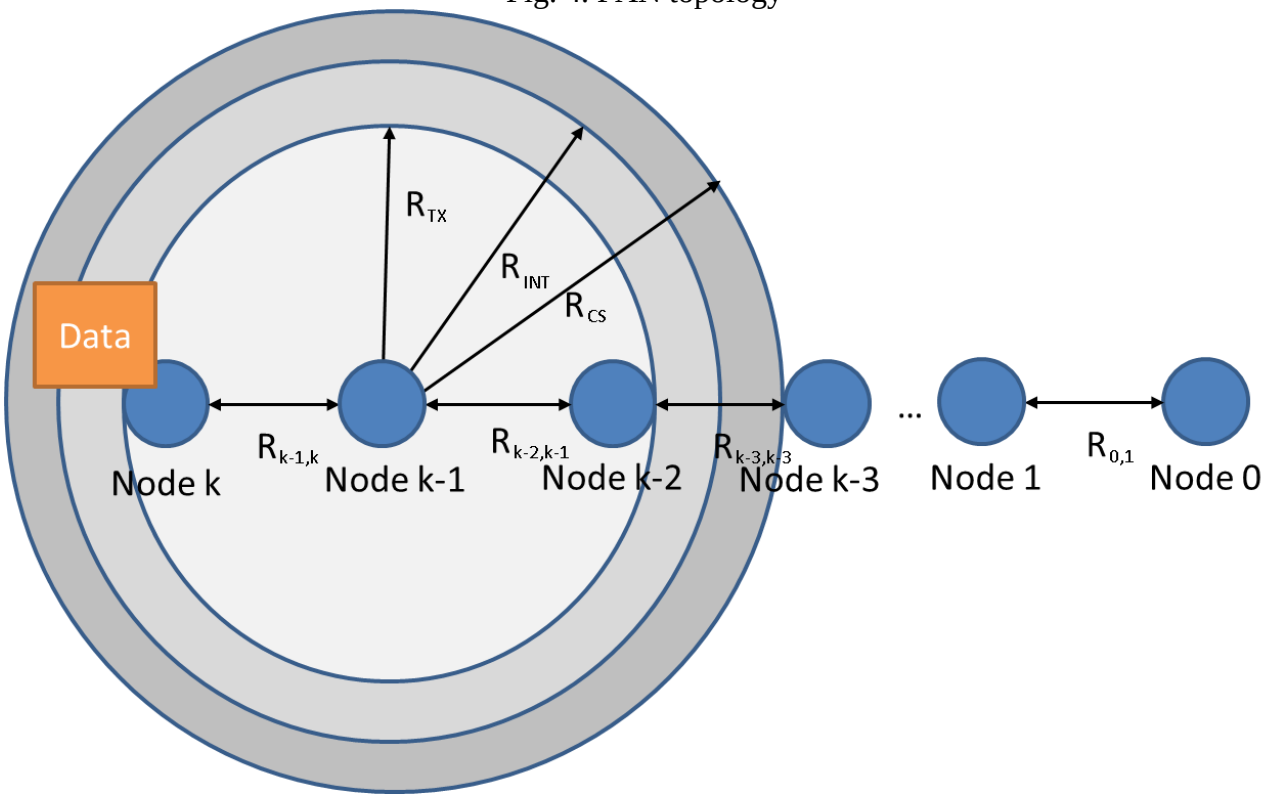

Fig. 5. Frame transmission phases for IEEE 802.15.4 beacon-enabled (CAP and CFP) and nonbeacon-enabled PANs

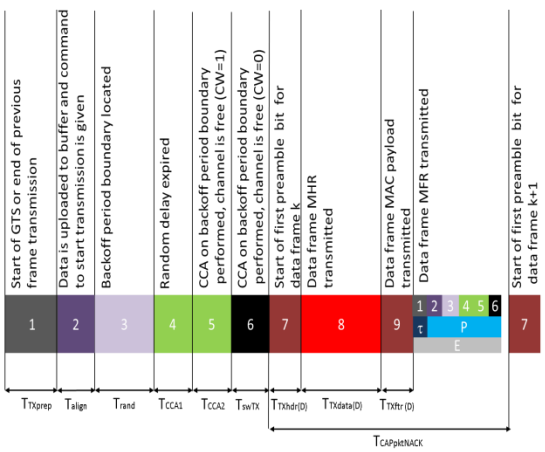


a) Unacknowledged transmission in CAP

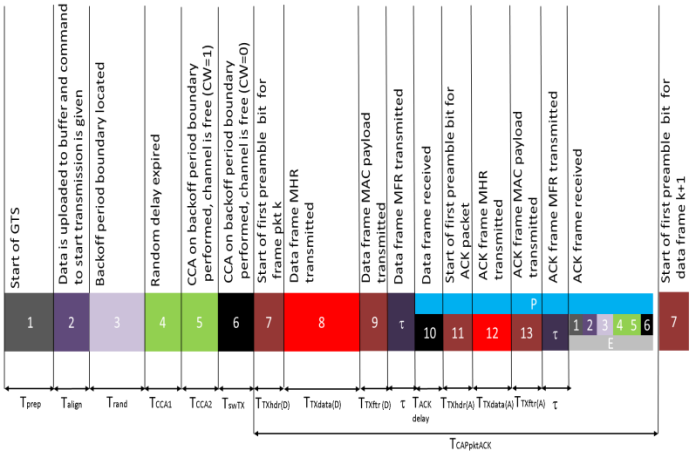


b) Acknowledged transmission in CAP

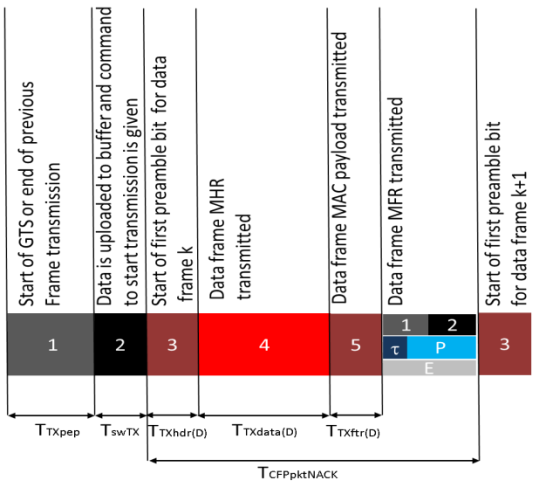


c) Unacknowledged transmission in CFP

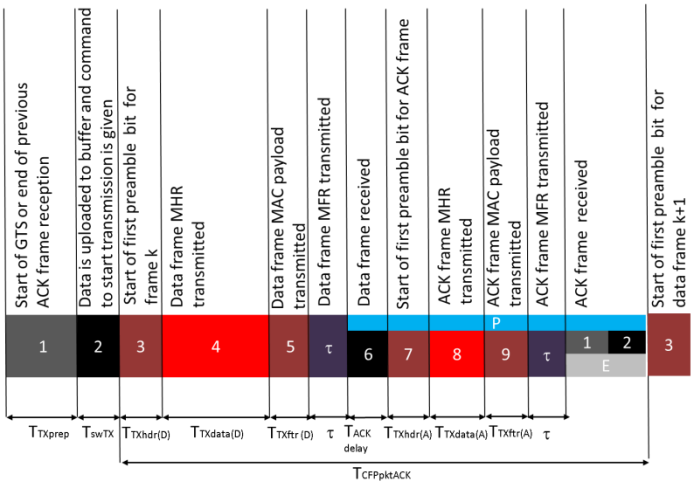


d) Acknowledged transmission in CFP

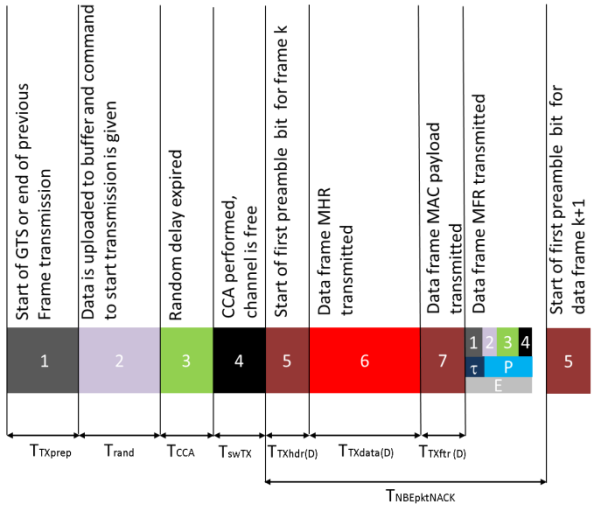


e) Unacknowledged transmission in nonbeacon-enabled PAN

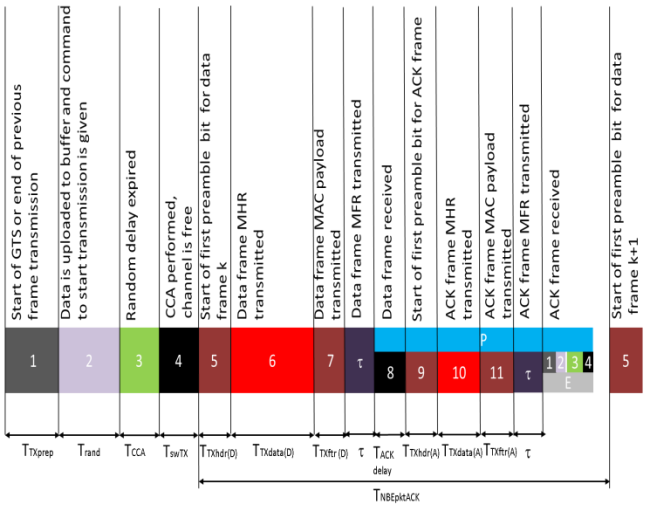


f) Acknowledged transmission in nonbeacon-enabled PAN

Fig. 6. Effect of payload and frame processing time on the maximum MAC-level throughput during CAP in IEEE 802.15.4 beacon-enabled PAN with 2450 DSSS PHY (τ=0) (analytic result)

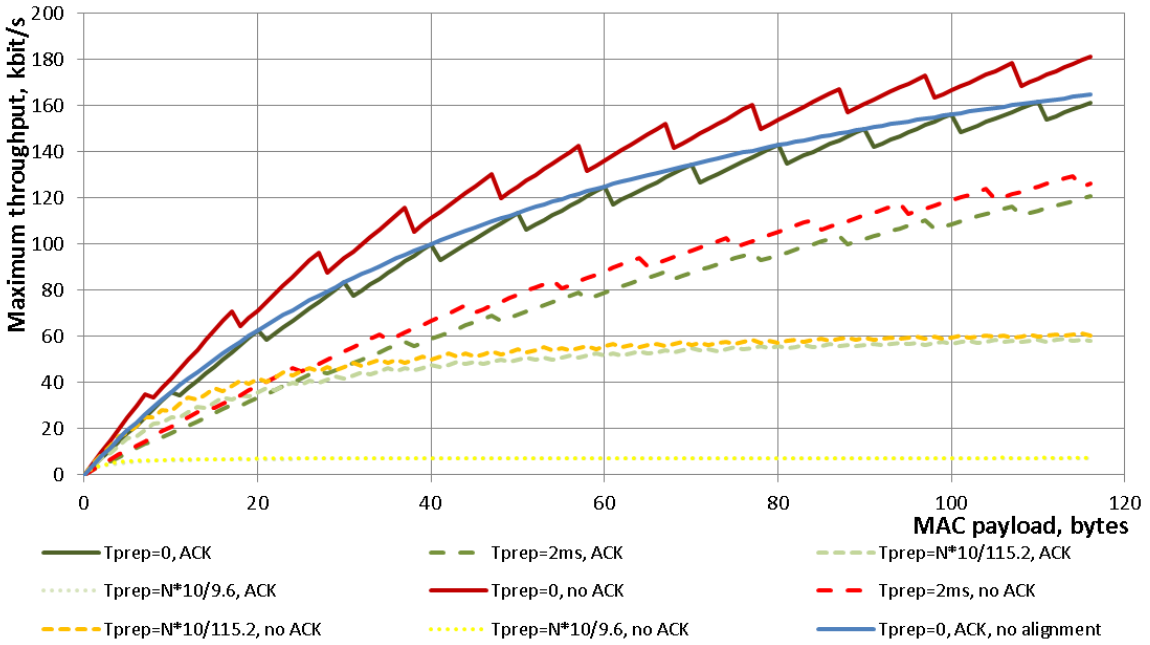


Fig. 7. Effect of payload and frame processing time on the maximum MAC-level throughput during CFP in IEEE 802.15.4 beacon-enabled PAN with 2450 DSSS PHY (τ=0) (analytic result)

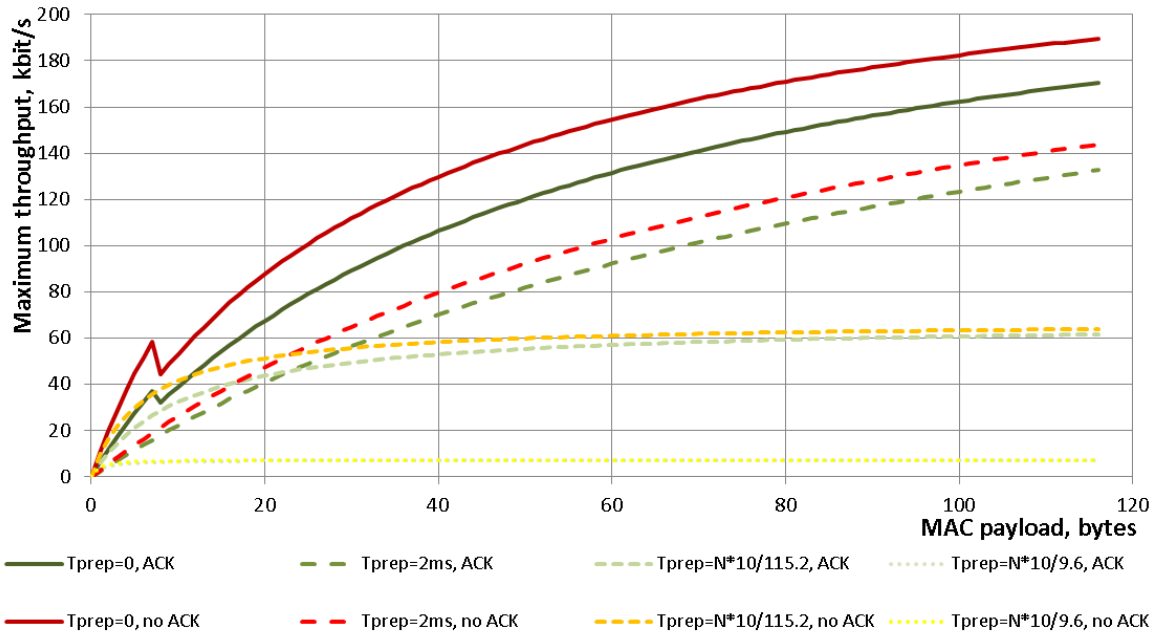

Fig. 8. Effect of payload and frame processing time on the maximum data throughput in IEEE 802.15.4 nonbeacon-enabled PAN with 2450 DSSS PHY (τ=0) (analytic result)

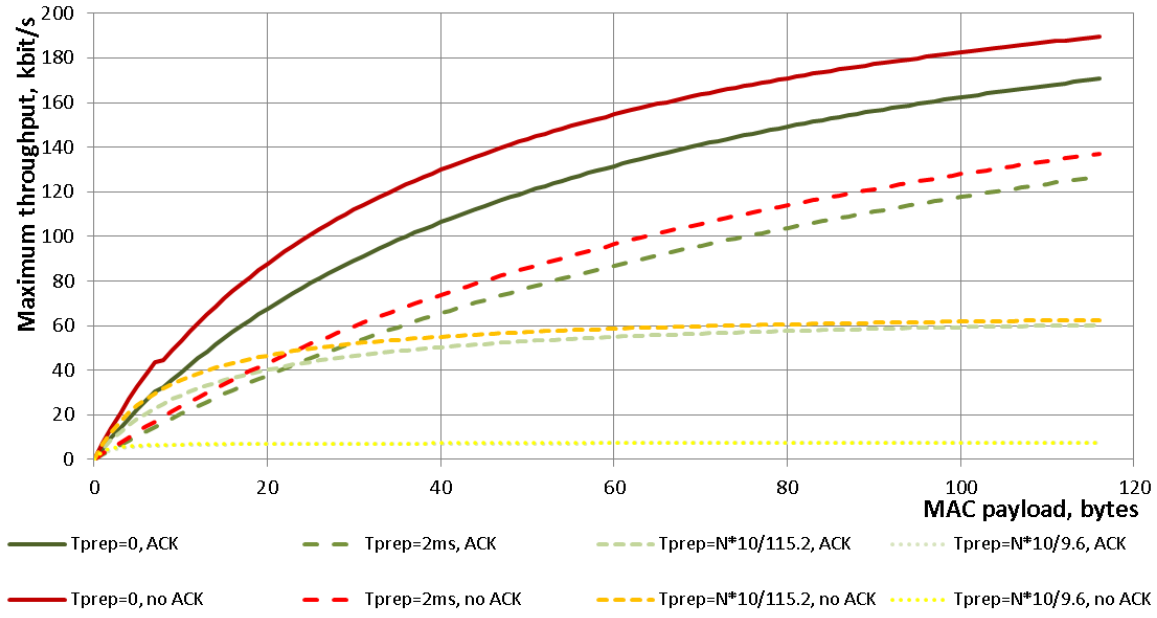


Fig. 9. The relationship between incoming (received) and outgoing (transmitted) beacon for a coordinator in IEEE 802.15.4 beacon-enabled PAN [32]

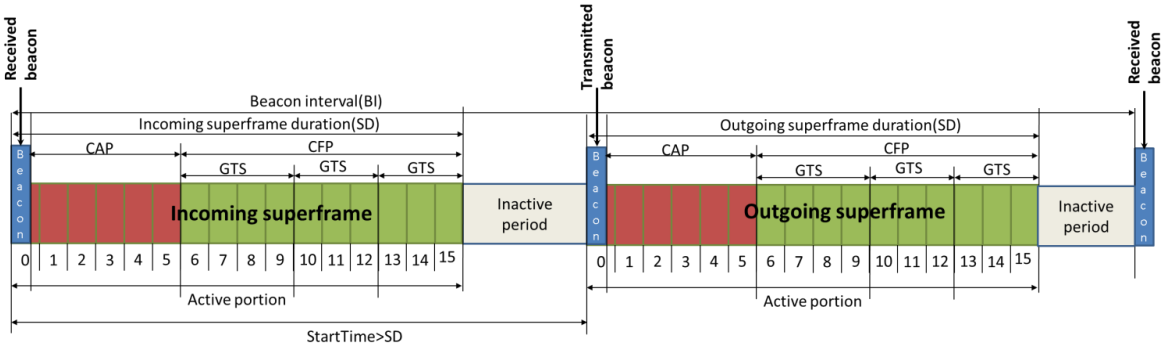

Fig. 10. Maximum data streaming throughput in multihop IEEE 802.15.4 beacon-enabled PAN with 2450 DSSS PHY (analytic result)

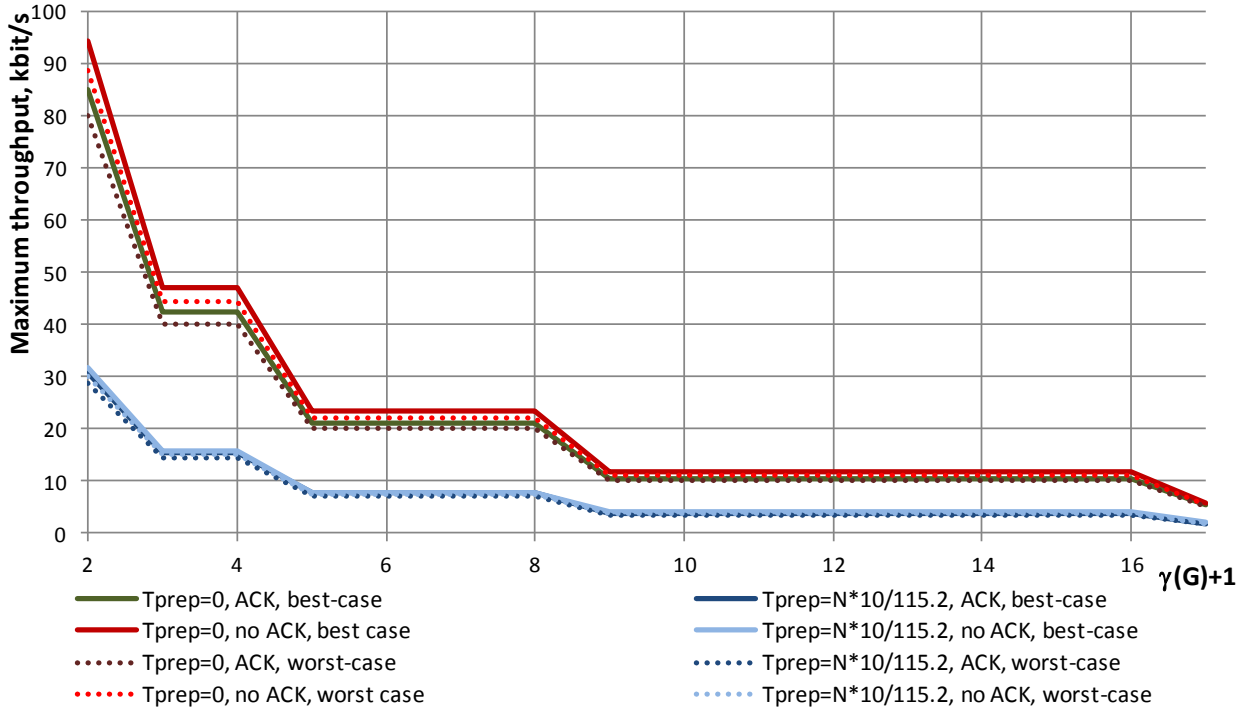


Fig. 11. Maximum data streaming throughput in multihop IEEE 802.15.4 nonbeacon-enabled PAN with 2450 DSSS PHY (analytic result)

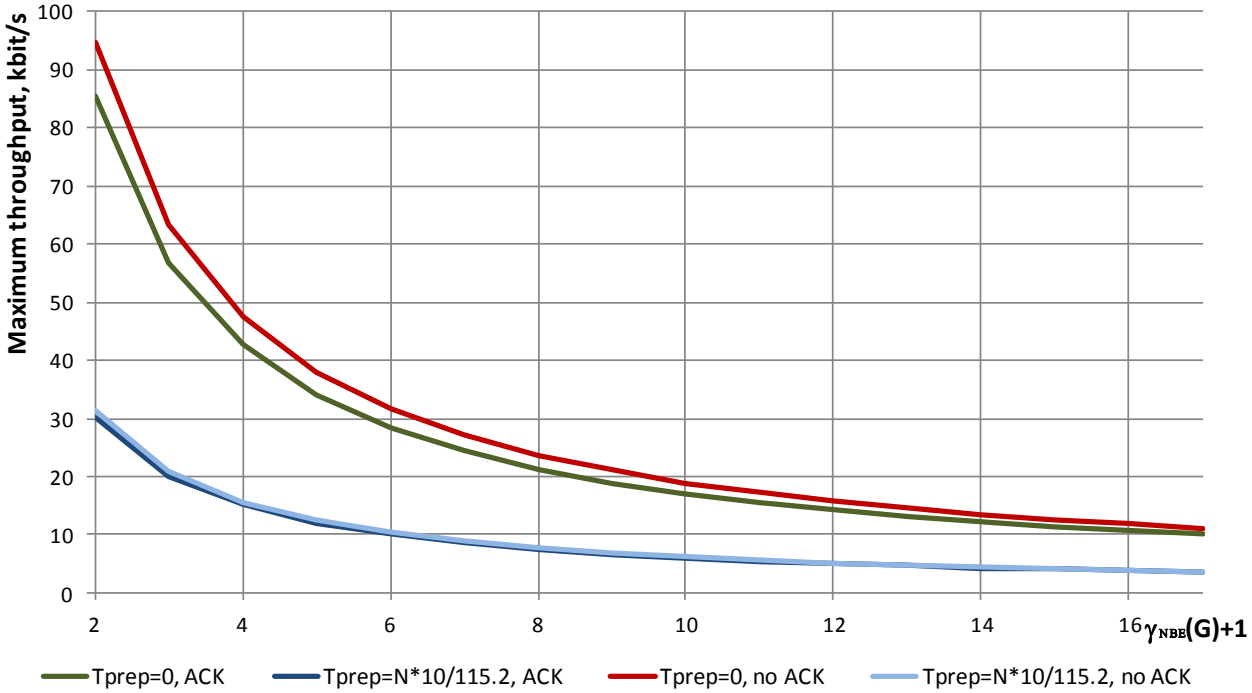

Fig. 12. Maximum data streaming throughput for different operation modes in IEEE 802.15.4 PAN with 2450 DSSS PHY (experimental result)

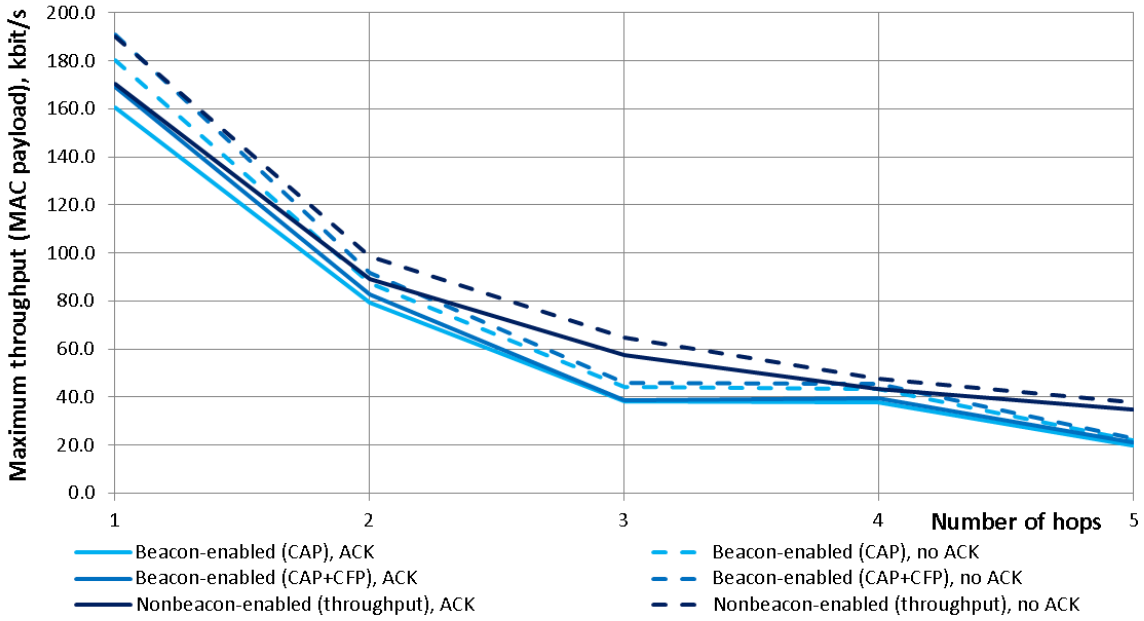


Fig. 13. Average end-to-end latency for five hop data transfer for different operation modes in IEEE 802.15.4 PAN with 2450 DSSS PHY (experimental result) *(BO=SO+3)*

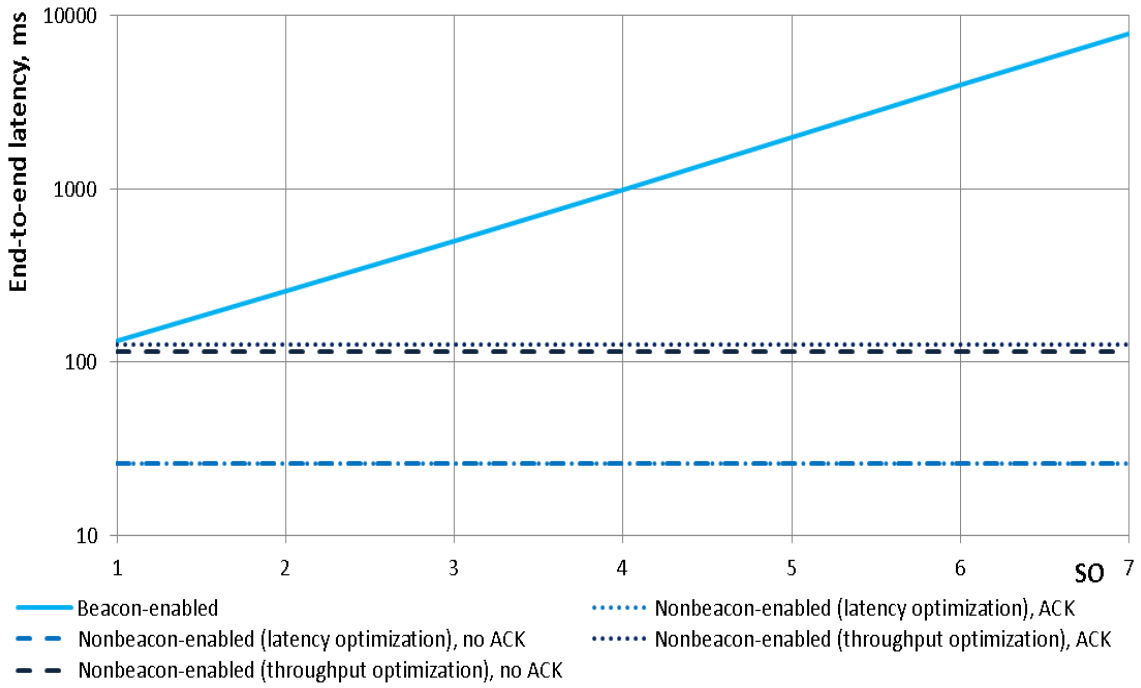

Fig. 14. Effect of SO on the number of data frames transmitted by node 4 in 5-hop network (experimental result) *(Note: number of received frames is always 1000, BO=SO+3)*

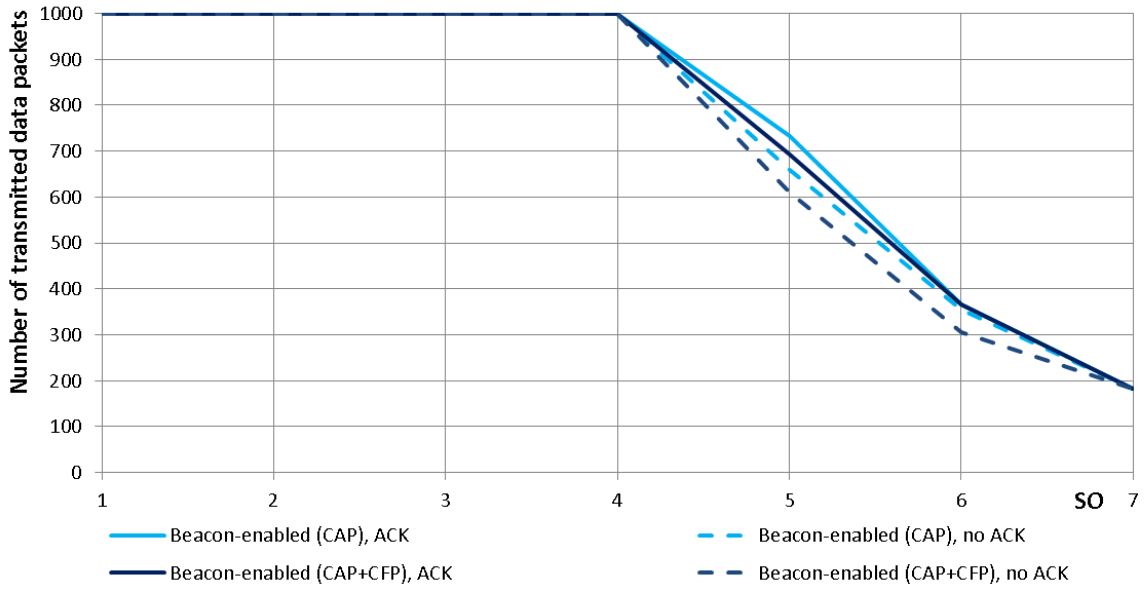


Fig. 15. Effect of SO and frame payload size on the maximum throughput over beacon-enabled IEEE 802.15.4 single hop PAN (experimental result) *($N_{CAP}$=1, $N_{CFP}$=15, BO=SO)*

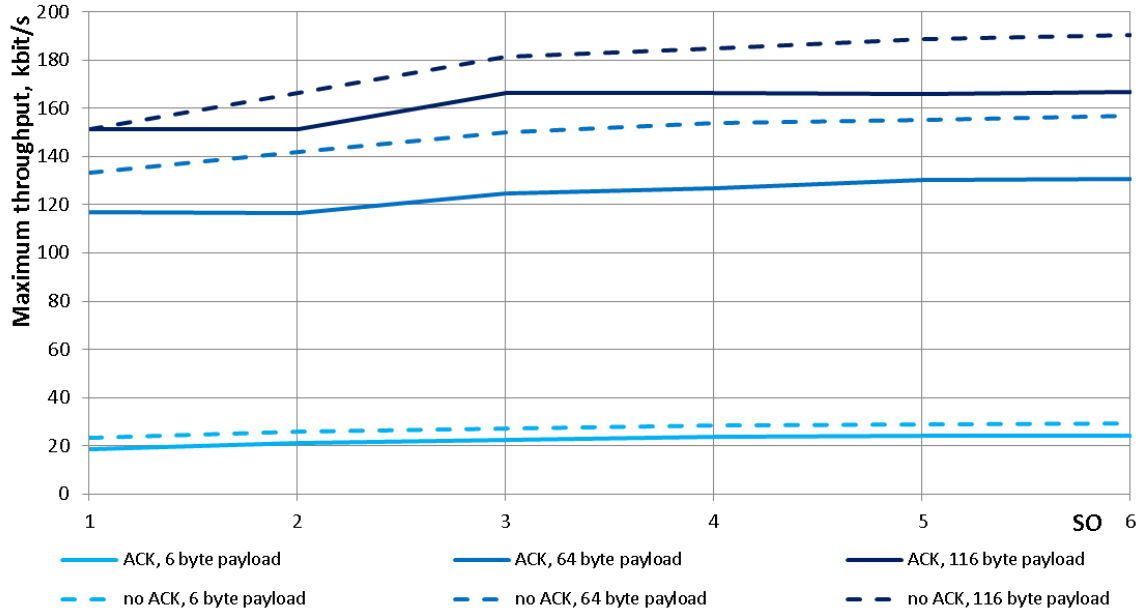

Fig. 16. Effect of SO on the maximum throughput over 5-hop beacon-enabled IEEE 802.15.4 PAN (experimental result) *(BO=SO+3)*